Film Profiles Behind Liquid Slugs in Gas-Liquid Pipe Flow

Martin Cook and Masud Behnia
School of Mechanical and Manufacturing Engineering, University of New South Wales, Sydney, Australia 2052

A comprehensive one-dimensional fully coupled hydrodynamic treatment of the film profiles behind liquid slugs in horizontal and inclined gas–liquid slug flow is presented. Experiments were performed in horizontal air–water pipes 32 and 50 mm in diameter, the smaller also being inclined to an angle of 5 degrees. Time traces of film thickness were produced with the use of a wire-probe technique. The experimental results are compared against the theory presented here, as well as previously reported hydrodynamic models. It is concluded that the film profiles calculated by the use of one-dimensional models are highly sensitive to the choice of input variables, for example, the slug translational velocity; however, good agreement is achievable provided that consistent hydrodynamic equations and correct input variables are used. It is hoped that the work presented here will influence future mechanistic models of slug flow.

Introduction

When a gas and a liquid flow concurrently in a pipe a number of different flow patterns or regimes may be present, depending largely on the superficial velocities of both phases. The slug-flow regime is found commonly in crude oil/gas multiphase pipelines, boiler tubes, and heat exchangers. It is initiated when waves of a stratified liquid layer grow until they reach the top of the pipe. Once this has occurred the gas propels a "slug" of liquid rapidly down the pipe. Immediately preceding the slug, liquid is scooped up from the stratified liquid film layer, while behind the slug the liquid level drops until the whole process is repeated. The slug length becomes stable as the rate of liquid picked up from the preceding film equals the rate of liquid shed at the rear of the slug. The resulting flow pattern is a series of liquid slugs with some aeration, separated by a liquid film, as shown in Figure 1.

In the early work of Dukler and Hubbard (1975) the film was treated as an uncoupled free surface channel flow. The nature of the film was investigated by considering a momentum balance on the film with respect to a frame of reference that moves down the pipe at the speed of the slug. Dukler and Hubbard based their model on the observation that a constant flux of fluid moves through the slug and into the trailing film, hence the average velocity of fluid in the slug was taken to be somewhat less than the speed of the slug itself. Their one-dimensional approach has formed the basis of all models since.

Nicholson et al. (1978) extended the model of Dukler and Hubbard to cover the entire intermittent two-phase flow regime, and modified their hydrodynamic treatment of the film that was found to predict rising, rather than falling, film levels behind slugs under certain flow conditions. Various simplified approaches have been suggested in which the film height is assumed constant at its equilibrium level, including the long slug model of Andreussi et al. (1993), or the film shape is calculated to find the film height at the end of the film, and this value is used as the constant film height in all subsequent calculations (Nicholson et al.,1978).

All models require empirical correlations for the necessary inputs of slug liquid holdup, slug frequency or length, and slug translational velocity, all of which affect the shape and length of the film between liquid slugs. Experimental and theoretical investigations of these parameters are summarized well by Taitel and Barnea (1990b). Additionally, all ex-

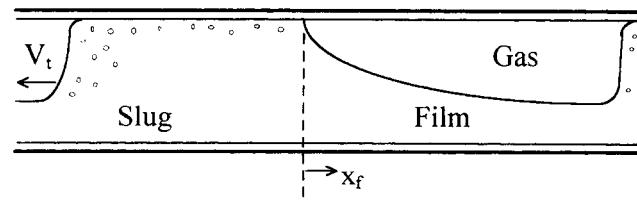

Figure 1. Basic slug-flow model.

isting models use established single-phase wall-friction-factor correlations in the film regions where a stratified flow is present. Where gas effects have been considered, existing interfacial friction factors for rough interfaces developed for stratified flow have been employed.

The work presented in this article is concerned with the shape and length of the film that trails each slug. It is the film shape that determines, from continuity requirements, the length of the slug body and film, as well as the velocity profile along the liquid film. These are necessary to calculate the pressure gradient, heat, and mass-transfer rates. A correct hydrodynamic treatment of the film is thus central to existing mechanistic models of slug flow that seek to predict pressure gradients and liquid holdup. In this work the theory is generalized to include the coupling between the gas and liquid phases, and the results compared with measurements made of film thickness in order to validate the model and parameters used in the calculations.

Film Hydrodynamics

In both the horizontal and inclined orientations the flow consists of an elongated bubble above the liquid film, as shown in Figure 1. Generally it is assumed that this liquid film contains no dispersed bubbles along its length. The average liquid velocity in the slug is V_s, and the velocity of the dispersed bubbles in the slug is given as V_b. Both these velocities are somewhat less than the velocity at which the elongated bubble and the slug move downstream, V_t. The liquid velocity in the film decreases as the film height is reduced away from the preceding slug. Conversely, the velocity of the gas in the film zone increases as the void fraction increases.

Fully comprehensive momentum balance equations will be developed for both the gas and liquid phases, in a frame of reference that moves with the slug and bubble. Such a moving coordinate system eliminates any transient terms from the equations, leaving a steady problem to be solved. The forces acting on the fluid elements are shown in Figure 2, where P_G and P_L are the average pressures for the gas and liquid. The hydrostatic pressure of the gas is neglected; however, for the liquid the average pressure is given by

$$P_L = P_G + \rho_L g \xi D \cos\beta, \tag{1}$$

where ξD is the depth at which the hydrostatic liquid pressure is calculated to yield the same result as the fully integrated solution. Here ξ is given in terms of the angle subtended by the liquid surface θ as

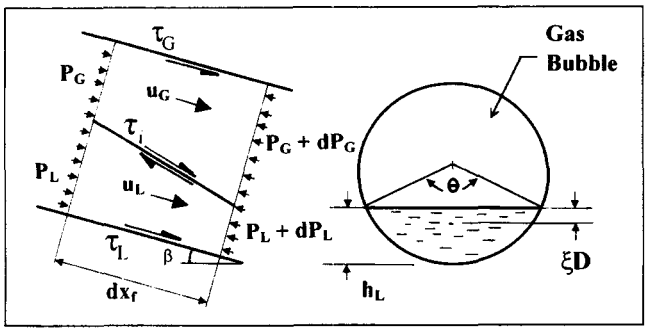

Figure 2. Flow geometry and forces.

$$\xi = \frac{2\pi}{3\pi(\theta - \sin\theta)}\sin^3\left(\frac{\theta}{2}\right) - \frac{1}{2}\cos\left(\frac{\theta}{2}\right). \tag{2}$$

The one-dimensional momentum balance equation for the liquid phase relative to a coordinate system that moves with the slug can now be written as

$$P_L A_L - (P_L + dP_L)(A_L + dA_l) + \tau_L S_L dx_f - \tau_i S_i dx_f + \rho_L g \sin\beta dx_f + \rho_L u_L^2 A_L - \rho_L u_L A_L (u_L + du_L) + \left(P_G + \frac{dP_G}{2}\right) dA_L = 0, \tag{3}$$

where u_L is the average liquid velocity at any point in the film zone relative to the moving coordinate system. The last term in Eq. 3 is the axial component of the pressure force acting on the inclined surface. Also, the wall shear stress term $\tau_L S_L dx_f$ is positive because in the moving frame the wall shear acts to speed up the flow.

The continuity requirement for the liquid phase is:

$$A_L du_L = -u_L dA_L. \tag{4}$$

Combining Eqs. 1, 3, and 4 and neglecting smaller order terms, yields

$$-A_L\frac{dP_L}{dx_f} + \tau_L S_L - \tau_i S_i + \rho_L u_L^2 \frac{dA_L}{dx_f} + \rho_L g \sin\beta - \rho_L g D \xi \cos\beta \frac{dA_L}{dx_f} = 0. \tag{5}$$

An equation is obtained in a similar manner for the gas, by treating it as incompressible and ignoring any hydrostatic gas pressure:

$$-A_G\frac{dP_G}{dx_f} + \tau_G S_G + \tau_i S_i - \rho_G u_G^2 \frac{dA_L}{dx_f} = 0. \tag{6}$$

Noting that

$$\frac{dA_G}{dx_f} = -\frac{dA_L}{dx_f}, \tag{7}$$

Eqs. 5 and 6 can be combined, together with a differentiated form of Eq. 1, to obtain a coupled momentum balance equation:

$$\frac{\tau_L S_L}{A_L} - \frac{\tau_G S_G}{A_G} - \tau_i S_i\left(\frac{1}{A_G} + \frac{1}{A_L}\right) + \frac{\rho_L g \sin\beta}{A_L} = \rho_L g D \cos\beta \frac{d\xi}{dx_f} + \frac{\rho_L g D \xi \cos\beta}{A_L}\frac{dA_L}{dx_f} - \left(\frac{\rho_L u_L^2}{A_L} + \frac{\rho_G u_G^2}{A_G}\right)\frac{dA_L}{dx_f}. \tag{8}$$

The first two terms on the RHS of Eq. 8 can be combined with the use of the product rule for differentiation, and expressed as follows:

$$\frac{\rho_L g D \cos\beta}{A_L}\left(A_L\frac{d\xi}{dx_f}+\xi\frac{dA_L}{dx_f}\right)=\frac{\rho_L g D\cos\beta}{A_L}\frac{d(A_L\xi)}{dx_f}. \quad (9)$$

Additionally,

$$\frac{d(A_L\xi)}{dx_f}=\frac{d(A_L\xi)}{d\theta}\frac{d\theta}{dA_L}\frac{dA_L}{dx_f}$$

$$=\left(\frac{\frac{\pi}{2}\left(\frac{\theta-\sin\theta}{2\pi}\right)\sin\left(\frac{\theta}{2}\right)+\sin^2\left(\frac{\theta}{2}\right)\cos\left(\frac{\theta}{2}\right)}{1-\cos\theta}-\frac{1}{2}\cos\left(\frac{\theta}{2}\right)\right)\times\frac{dA_L}{dx_f}. \quad (10)$$

Using Eqs. 8, 9 and 10 and the trigonometric relation $1-\cos\theta=2\sin^2(\theta/2)$, an expression for the change in liquid holdup along the film can be obtained as

$$\frac{dA_L}{dx_f}=\frac{\frac{\tau_L S_L}{A_L}-\frac{\tau_G S_G}{A_G}-\tau_i S_i\left(\frac{1}{A_G}+\frac{1}{A_L}\right)+\frac{\rho_L g\sin\beta}{A_L}}{\frac{\rho_L g D\cos\beta}{A_L}\left(\frac{\theta-\sin\theta}{8\sin\left(\frac{\theta}{2}\right)}\right)-\frac{\rho_L u_L^2}{A_L}-\frac{\rho_G u_G^2}{A_G}}. \quad (11)$$

Dukler and Hubbard (1975) and Nicholson et al. (1978) have both derived equations for the film profile based on an uncoupled free-surface approach, and their equations are equivalent to Eq. 11 if the gas and interfacial terms were to be neglected. Equation 11 can be expressed in terms of film height by using:

$$\frac{dA_L}{dx_f}=S_l\frac{dh_L}{dx_f}, \quad (12)$$

where S_l is the interfacial length. Equation 11 can be manipulated with the use of the following relations

$$A_L=\frac{\pi D^2}{4}\left(\frac{\theta-\sin\theta}{2\pi}\right), \qquad S_l=D\sin\frac{\theta}{2} \quad (13)$$

to yield an expression for the change in film thickness with distance from the preceding slug:

$$\frac{dh_f}{dx_f}=\frac{\frac{\tau_L S_L}{A_L}-\frac{\tau_G S_G}{A_G}-\tau_i S_i\left(\frac{1}{A_G}+\frac{1}{A_L}\right)+\rho_L g\sin\beta}{\rho_L g\cos\beta-S_i\left(\frac{\rho_L u_L^2}{A_L}+\frac{\rho_G u_G^2}{A_G}\right)} \quad (14)$$

Taitel and Barnea (1990a) have developed a similar equation for the film shape. However, their derivation differs from the approach taken here, where we treat the pressure gradient in each phase separately. A film profile equation can also be developed using the same comprehensive approach as here, in which the hydrostatic pressure in the gas region is not neglected. The net result of this rather involved procedure is an equation identical to Eq. 14, with the exception that the hydrostatic terms in both the numerator and denominator of Eq. 14 are in terms of $(\rho_L-\rho_G)$ rather than just ρ_L.

The analysis thus far has involved only the relative velocities u_L and u_G. However, the shear stress terms are functions of the absolute fluid velocities as follows:

$$\tau_L=f_L\rho_L\frac{|V_t-u_L|(V_t-u_L)}{2} \qquad \tau_G=f_G\rho_G\frac{|V_t-u_G|(V_t-u_G)}{2}$$

$$\tau_i=f_i\rho_G\frac{|u_L-u_G|(u_L-u_G)}{2}, \quad (15)$$

where the fluid friction factors can be determined by the Blasius relation based on the following Reynolds numbers:

$$Re_L=\rho_L|V_t-u_L|D_L/\mu_L \qquad Re_G=\rho_G|V_t-u_G|D_G/\mu_G, \quad (16)$$

with $D_L=4A_L/S_L$ and $D_G=4A_G/(S_G+S_i)$. A constant value for the interfacial friction factor has been used by Shoham and Taitel (1984) for wavy stratified flow, and their value of $f_i=0.014$ is used for all calculations. Further, relations for the geometrical parameters A_L, S_L, A_G, S_G, S_i and liquid holdup as a function of film height for circular pipes may be found in Taitel and Dukler (1976) or Taitel and Barnea (1990b).

In order to calculate the film shape it is necessary to set the initial film height and liquid velocity. The film height is set such that the initial film holdup equals the holdup in the slug. The initial velocity of the liquid in the film is assumed to be equal to the average velocity of the liquid in the preceding slug, V_s. Applying a continuity balance to the flow of both gas and liquid within the slug yields:

$$V_m=j_L+j_G=V_S E_{LS}+V_b(1-E_{LS}). \quad (17)$$

Clearly for an all-liquid slug the average liquid velocity will equal the flow-mixture velocity, V_m. The dispersed bubble velocity, V_b, depends on the distribution of bubbles within the slug. For relatively high flow rates the slug is highly aerated with the bubbles distributed uniformly across the pipe diameter, so that $V_b\approx V_S$. For low flow rates the average gas velocity in the slug will be somewhat less than the average liquid velocity, as the dispersed bubbles congregate near the top of the pipe wall. However, at such flow rates the aeration of the slug is very low, making the last term of Eq. 17 negligible. It can thus be expected that the average velocity of liquid in the slug is approximated well by the flow mixture velocity over a wide range of input flow rates, and hence the flow-mixture velocity is used as the initial film liquid velocity.

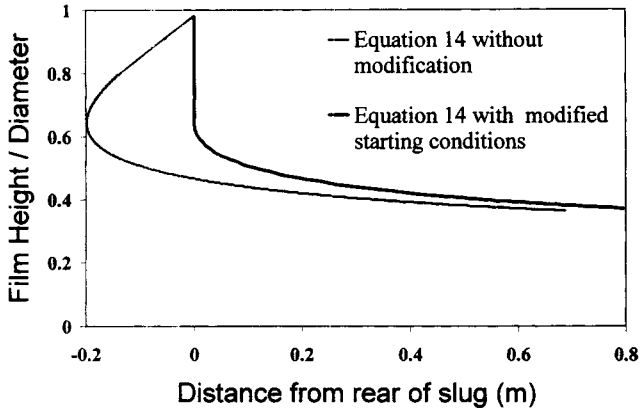

Figure 3. Effect of altering film starting conditions.

For flow below a certain critical mixture velocity the film gradient predicted by Eq. 14 may be positive, leading to a film shape that curves backwards into the body of the slug. Such unrealistic solutions are avoided by reducing the initial film liquid level until dh_f/dx_f becomes negative. This effect is illustrated in Figure 3 for a low mixture velocity flow, where it can be seen that the effect of altering the film starting conditions diminishes quickly along the length of the film. This procedure results in an instantaneous fall in the liquid holdup from the value of the holdup in the slug to the critical initial film value, and has been noted by Taitel and Barnea (1990b) to resemble drainage into a supercritical channel flow. The initial film velocities must also be adjusted to maintain continuity of both phases.

The overall length of the film is determined by performing a mass balance along the length of the film until continuity requirements are satisfied. Previous researchers, such as Dukler and Hubbard (1975) and De Henau and Raithby (1995), have applied the simplification that the film height is constant in carrying out the mass balance. The present results show that this simplification can have a significant effect on the predicted film length and average liquid holdup, especially if the film is short.

Wire-Probe Measurement of Film Profile

The use of an electrically conducting liquid phase allows the variation of film thickness behind a slug to be recorded by measuring the conductance between two electrodes. In order to achieve highly localized measurements of the film height at the center of the pipe, two wire electrodes were stretched across the pipe diameter. An oscillating current was applied to the probe to give a linear voltage response vs. liquid height.

The behavior of such probes has been investigated by Brown et al. (1978), who showed that the sensitivity is increased by using higher frequency excitation. They suggested a minimum excitation frequency of 1 kHz, below which some long-term drift in the impedance of the device was noted. Sufficient sensitivity to measure slug film profiles was achieved by using a 6-kHz excitation. The calibration of the probe was continually checked throughout the course of the experiments to detect drift, and very little drift was noticed.

Wire probes have been used previously to measure film thickness in annular flows by Miya et al. (1971). The intermittent nature of slug flow, however, means that the probe is continually immersed in the high-speed liquid phase of the slug, followed by the mostly gaseous bubble region. This cyclic process allowed air to get trapped behind the wires, which affected the value and steadiness of the probe output. The use of 0.5-mm flat stainless-steel wires was found to eliminate this problem and minimize the effect of the probe on the flow. Further, as the probe passes through the falling liquid film, it can be expected that a thin layer of water adheres to the wires indicating a film height somewhat higher than is actually the case. Brown et al. (1978) have reported that such probes have been used to measure very high-speed wave disturbances where this time-lag effect was shown to be negligible.

For all but the fastest and most aerated slugs, the probe could be used to estimate the holdup in the slug itself. Toward the rear of the slug the dispersed bubbles were observed to coalesce at the top of the pipe, creating an effectively stratified section of flow. With this known distribution of gas in the slug, holdup in the slug could be measured.

Experiments

Tests were conducted in two 16-m-long, smooth Perspex pipes of 32 and 50 mm ID, over a range of mixture velocities from 1.0 m/s to over 8 m/s. The pipelines were attached to a supporting truss that could be inclined, allowing both horizontal and upward flow to be analyzed. Experiments were conducted in both pipes in the horizontal configuration, and data were also collected in the smaller pipe at an inclination of five degrees. All experiments used air and water as the gas and liquid phases, respectively. The pipes were constructed of 2-m-long sections that could be easily removed and reinstalled. One of these sections in each pipe, the test section, contained the wire probe and two impact tubes, whose dynamic pressure response was used to detect the front and rear of a slug. An analysis of the impact tube response also enabled slug speed, length, and frequency to be determined.

Air and water entered the pipes via a mixing nozzle at the inlet to each pipe, and the test section was located 10 m from the inlet, allowing a sufficient length for slugs to form and grow before they entered the test section. A further 4 m was kept between the test sections and outlet, due to the transient pressure fluctuations that occur when a slug exits the pipe into the separator at atmospheric conditions. It was found that these pressure fluctuations, which result in a sudden increase in the speed of the following slug, did not affect the test-section readings significantly.

The water was circulated in a closed loop by a centrifugal pump. Air was supplied from a high-pressure line, and both phase flow rates were measured with standard orifice plates. A venturi was also used in the case of higher water flow rates.

Results and Discussion

At each set of flow rates investigated, film profiles were measured behind a large number of slugs, provided that the preceding slug was of sufficient length to ensure that the velocity profile at the rear of the slug was fully developed. Barnea and Taitel (1993) note that short slugs are unstable and collapse as a result of the lack of development of such a velocity profile. As the analysis discussed thus far is based on

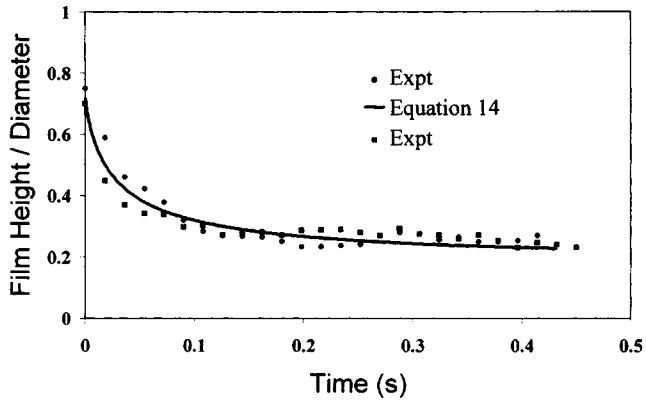

Figure 4. Time trace of film profile ($\beta = 0$; $D = 32$ mm; $j_L = 1.51$ m/s; $j_G = 4.11$ m/s).

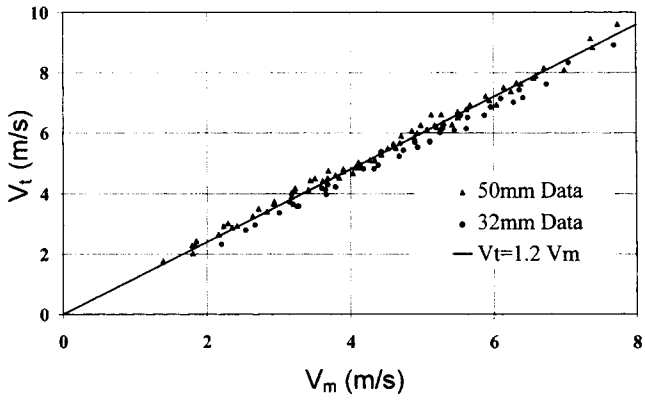

Figure 6. Slug transitional velocity vs. flow-mixture velocity for horizontal flow.

stable flow with no growth or collapse of slugs, only the profiles behind relatively long slugs were investigated.

At a selection of flow rates two typical film profiles have been measured, and samples are shown in Figures 4 through 8. As can be readily seen in these figures, the measured profile shapes are consistent regardless of the intermittent nature of the flow. Very little difference between profile shapes was observed for profiles measured at the same flow rates, although the overall length of the films vary considerably. The calculated film lengths are average lengths, so it is expected that the individually measured film lengths need not be in close agreement with the calculations. Indeed, most of the measured film lengths are somewhat longer than the predictions, as a result of the choice of relatively long slugs.

It was found that the shape of the calculated profiles were highly sensitive to the value of V_t used in the calculations. Other investigators, such as Shemer and Barnea (1987) and Nicklin et al. (1962), have suggested that the slug translational velocity is equal to the center-line liquid velocity in the slug. This velocity is very close to 1.2 times the mixture velocity for a fully turbulent velocity profile in a pipe. It was found that using Eq. 14 and this value for V_t resulted in very good agreement between the experimental and calculated results over a wide range of flow rates. This relationship for V_t has been used in all calculations except where indicated. Figure 5 shows profiles predicted by Eq. 14 with V_t calculated as before, and with the correlation used by Dukler and Hubbard (1975). Clearly, for a slight difference in the input value of V_t, the profile shape differs considerably. Slug translational velocity was measured directly during the experiments, and Figure 6 shows that our data supports this linear relationship between V_t and V_m.

In the model of Taitel and Barnea (1990b) the slug translational velocity was taken to be a function of both the mixture velocity and a drift-velocity term. Horizontal drift was explained by Bendiksen (1984) to be due to the effect of elevation differences along the bubble nose, and was calculated to be a function of pipe diameter only, such that

$$U_d = 0.542\sqrt{gD}\,. \tag{18}$$

Figures 7 shows that the model of Taitel and Barnea (1990a) predicts higher film heights than experimentally observed, which also leads to longer film lengths and hence a substantially different prediction of various flow parameters.

Bendiksen (1984) noted that as the velocity of the bubble increases, the nose of the bubble becomes centralized, presumably eliminating the elevation differences in the bubble

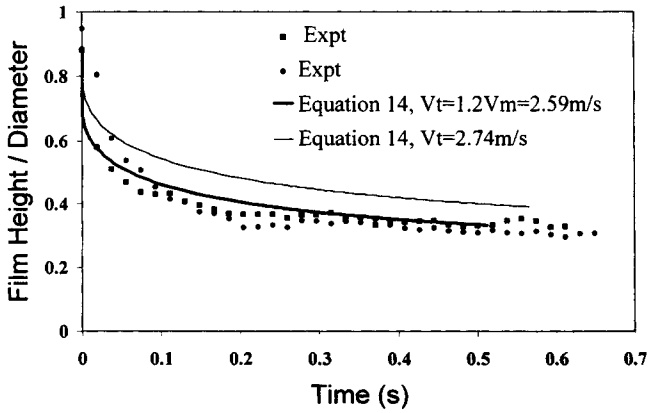

Figure 5. Time trace of film profile ($\beta = 0$; $D = 50$ mm; $j_L = 1.00$ m/s; $j_G = 1.16$ m/s).

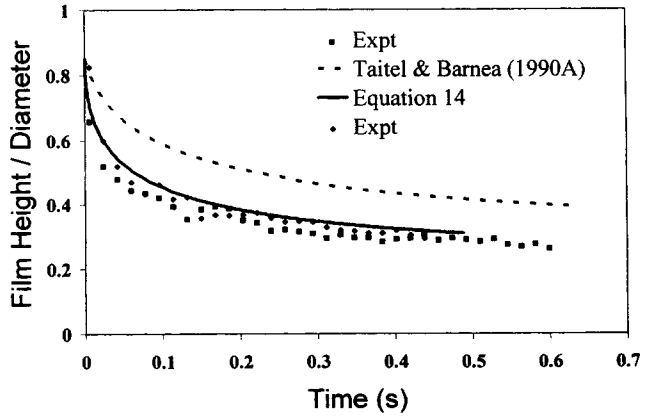

Figure 7. Time trace of film profile ($\beta = 0$; $D = 50$ mm; $j_L = 1.42$ m/s; $j_G = 2.08$ m/s).

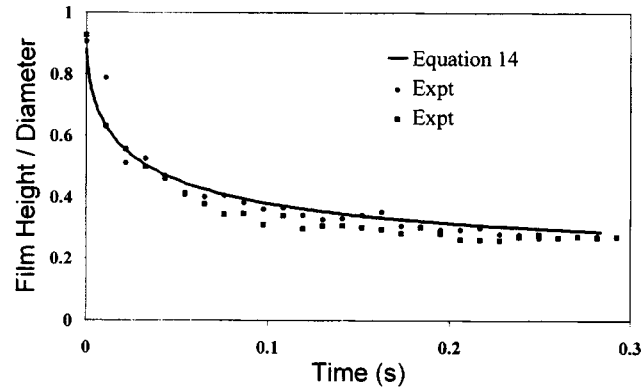

Figure 8. Time trace of film profile for inclined flow ($\beta = +5$; $D = 32$ mm; $j_L = 1.40$ m/s; $j_G = 2.00$ m/s).

nose and any drift-velocity component. Our direct measurements of V_t suggest that this drift component need not be considered at the velocities investigated here, which cover almost the full range at which the slug-flow regime exists, regardless of pipe diameter.

In order to achieve computational simplicity, other investigators, such as Nicholson et al. (1978) and Dukler and Hubbard (1975), have calculated the length of the film based on the assumption of a constant film height. In their models the level and velocity of fluid in the film zone are constant and equal to the values obtained from the integration of the film momentum equations at the end of the film. This simplification is not trivial, as shown in Figure 9, where it can be seen that the average liquid holdup along the film in our experiments is about 1.4 times the holdup at the end of the film for all mixture velocities. Thus, a constant film-height approximation leads to significantly shorter films than the complete solution, as noted by Andreussi (1993).

All calculations of film profiles have used the measured holdup at the rear of the preceding slug as the initial film holdup. Previous slug-flow models have all assumed that the initial holdup in the film is equal to the average holdup in the preceding slug. It was found that the difference in the two approaches could be significant at high mixture velocities, when the axial variation in holdup along the slug is considerable.

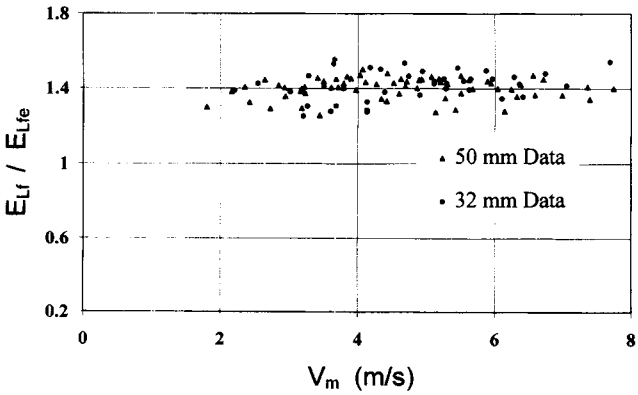

Figure 9. Ratio of average film holdup to film-end holdup for all mixture velocities ($\beta = 0$).

The film profile behind a slug of subcritical mixture velocity is shown in Figure 5. Although the one-dimensional approach presented here is not expected to accurately predict the shape of the film close to the nose of the bubble, it can be seen that the simple technique of applying an instantaneous fall in the calculated film height agrees well with the measured film shape. The critical mixture velocity was found to be approximately 3 m/s in both pipes, which was near the lower limit of mixture velocity for slugging to occur.

The upwards inclination of the pipeline produced film profiles that fell behind the slug far more rapidly than in the equivalent horizontal flow. This effect resulted in considerably shorter films, and hence a general increase in the slugging frequency for positively inclined flow. Figure 8 shows that the profile predicted by Eq. 14 matches well with a typical measured profile for flow at a +5-degree inclination. Interestingly, the translational velocity of the slugs was unaffected by a change in pipeline inclination. The slug speeds were consistently found to be equal to 1.2 times the flow mixture velocity over the range $1.0 < V_m < 8.0$ m/s in the 32-mm-diameter pipe.

Conclusions

Experiments have been performed in two air–water horizontal pipes of 32- and 50-mm diameter, and in the smaller pipe at a 5-degree inclination angle. The film profiles behind the slugs were measured using a wire probe. The results show a consistency in the shape of the liquid profiles, and it has been possible to compare the results with the predictions of the theory presented here and an existing hydrodynamic model of slug flow.

The one-dimensional fully coupled hydrodynamic treatment of the film presented in this work is capable of accurately predicting the shape of the film profile behind slugs over a range of flow conditions. The agreement between the theory and the measurements is sensitive to the choice of the slug translational velocity used in the calculations. This velocity has been measured to be consistently close to 1.2 times the flow mixture velocity, and this value gave calculated film profiles that agreed well with the measurements.

The accuracy of the one-dimensional approach seems to justify the use for single-phase friction factors in the film. It is not suggested, however that these friction factors are appropriate for the aerated body of the slug. It has been noted that the predicted length of the film may be significantly affected by the use of a constant film height assumption in the continuity calculations, which leads to a proportionally large change in the predicted slug length. Because this assumption does not lead to any great reduction in computational effort, its use is not recommended.

While the one-dimensional approach has been found to work well in the case of water, the use of oil as the liquid phase could be expected to lead to stronger two-dimensionality effects due to the higher viscosity.

Notation

A = cross-sectional area of pipe
D = pipe diameter
E_L = liquid holdup
f = friction factor

g = acceleration due to gravity
h_f = height of the liquid film
j = superficial velocity
l_f = length of the liquid film
S = wetted periphery
x_f = film distance parameter measured from start of film at slug trailing edge
β = pipeline inclination angle
ξ = nondimensionalized depth to the center of pressure of the film
ρ = density
θ = film geometry parameter (see Figure 2)

Subscripts

fe = end of film
f = film
t = translational

Literature Cited

Andreussi, P., A. Minervini, and A. Paglianti, "Mechanistic Model of Slug Flow in Near Horizontal Pipes," *AIChE J.*, **39**, 1281 (1993).

Barnea, D., and Y. Taitel, "A Model for Slug Length Distribution in Gas-Liquid Slug Flow," *Int. J. Multiphase Flow*, **19**, 829 (1993).

Bendiksen, K. H., "An Experimental Investigation of the Motion of Long Bubbles in Inclined Tubes," *Int. J. Multiphase Flow*, **10**, 467 (1984).

Brown, R. C., P. Andreussi, and S. Zanelli, "The Use of Wire Probes for the Measurement of Liquid Film Thickness in Annular Gas-Liquid Flows," *Can. J. Chem. Eng.*, **56**, 754 (1978).

DeHenau, V. and G. D. Raithby, "A Transient Two-Fluid Model for the Simulation of Slug Flow in Pipelines: I. Theory," *Int. J. Multiphase Flow*, **21**, 335 (1995).

Dukler, A. E., and M. G. Hubbard, "A Model for Gas-Liquid Slug Flow in Horizontal Tubes," *Ind. Eng. Chem. Fundam.*, **14**, 337 (1975).

Miya, M., D. E. Woodmansee, and T. J. Hanratty, "A Model for Roll Waves in Gas-Liquid Flow," *Chem. Eng. Sci.*, **26**, 1915 (1971).

Nicholson, M. K., K. Aziz, and G. A. Gregory, "Intermittent Two-phase Flow in Horizontal Pipes: Predictive Models," *Can. J. Chem. Eng.*, **56**, 653 (1978).

Nicklin, D. J., J. O. Wilkes, and J. F. Davidson, "Two Phase Flow in Vertical Tubes," *Trans. Inst. Chem. Eng.*, **40**, 61 (1962).

Shemer, L., and D. Barnea, "Visualization of the Instantaneous Velocity Profiles in Gas-Liquid Slug Flow," *Physicochem. Hydrodyn.*, **8**, 243 (1987).

Shoham, O., and Y. Taitel, "Stratified Turbulent-Turbulent Gas Liquid Flow in Horizontal and Inclined Pipes," *AIChE J.*, **30**, 377 (1984).

Taitel, Y., and A. E. Dukler, "A Model for Predicting Flow Regime Transitions in Horizontal and Near Horizontal Gas-Liquid Flow," *AIChE J.*, **22**, 47 (1976).

Taitel, Y., and D. A. Barnea, "A Consistent Approach for Calculating Pressure Drop in Inclined Slug Flow," *Chem. Eng. Sci.*, **45**, 1199 (1990a).

Taitel, Y., and D. A. Barnea, "Two-Phase Slug Flow," *Adv. Heat Transfer*, **20**, 83 (1990b).

Manuscript received Oct. 16, 1996, and revision received Apr. 18, 1997.